



Fluorescence spectral detection of copper(II), mercury(II) and zinc(II) based on a multifunctional peptide-based sensor

Lianshun Zhang, Shuaibing Yu, Lei Gao, Wei Meng, Chen Fu & Lianzhi Li

To cite this article: Lianshun Zhang, Shuaibing Yu, Lei Gao, Wei Meng, Chen Fu & Lianzhi Li (2022) Fluorescence spectral detection of copper(II), mercury(II) and zinc(II) based on a multifunctional peptide-based sensor, Spectroscopy Letters, 55:7, 488-499, DOI: [10.1080/00387010.2022.2101477](https://doi.org/10.1080/00387010.2022.2101477)

To link to this article: <https://doi.org/10.1080/00387010.2022.2101477>



View supplementary material [↗](#)



Published online: 21 Jul 2022.



Submit your article to this journal [↗](#)



Article views: 35




View related articles [↗](#)



View Crossmark data [↗](#)



Fluorescence spectral detection of copper(II), mercury(II) and zinc(II) based on a multifunctional peptide-based sensor

Lianshun Zhang^a, Shuaibing Yu^a, Lei Gao^b, Wei Meng^a, Chen Fu^a and Lianzhi Li^a 

^aSchool of Chemistry and Chemical Engineering, Liaocheng University, Liaocheng, P. R. China; ^bZhong Yuan Academy of Biological Medicine, Liaocheng People's Hospital Affiliated to Shandong University, Liaocheng, P. R. China

ABSTRACT

A fluorescence peptide-based sensor (Dansyl-His-Thr-Glu-His-Trp-NH₂, D-P5) was synthesized by Fmoc solid phase peptide synthesis, using dansyl group as the fluorophore. The sensor exhibited different fluorescence responses and sensitive detections for copper(II), mercury(II) and zinc(II) ions as a multifunctional sensor. The detailed investigation suggested that the limits of detection were 37.6 nmol·L⁻¹, 37.8 nmol·L⁻¹ and 59.4 nmol·L⁻¹ for copper(II), mercury(II) and zinc(II) ions, respectively, and the highly sensitive sensor was not influenced by other species. The sensor exhibited a strong binding ability to copper(II), mercury(II) and zinc(II) ions with the binding constants of 3.23×10^5 L·mol⁻¹, 6.37×10^5 L·mol⁻¹ and 6.0×10^4 L·mol⁻¹, respectively. The binding stoichiometries of the sensor to copper(II), mercury(II) and zinc(II) ions measured by Job's plot were all 1:1. Furthermore, The sensor has been successfully used for the detections of copper(II), mercury(II) and zinc(II) in actual water samples.

ARTICLE HISTORY

Received 18 April 2022
Accepted 7 July 2022

KEYWORDS



Copper(II); fluorescence spectroscopy; mercury(II); peptide sensor; zinc(II)


Introduction

With the continuous development of industrialization, various pollution problems have been brought, among which heavy metal ion pollution caused by industrial pollution is the most urgent.^[1] Due to the non-degradability and long-term accumulation of heavy metal ions, the accumulation of a large amount of heavy metal ions in the human body will cause various diseases.^[2–7] Copper is one of the most abundant transition metals in the human body, and is a trace element required by living organisms. However, excessive accumulation of Cu²⁺ results in many serious human afflictions, such as neurodegenerative diseases.^[8–11] Among the heavy and transition metal ions, mercury is considered to be a highly toxic metal ion, and its environmental pollution has brought serious problems to human health and ecology.^[12–15] Long-term exposure to mercury will damage the digestive organs, kidneys and endocrine system, etc.^[16–18] In addition, as the second most abundant transition metal ion in the human body, zinc plays an important role in maintaining activities in the body and

normal life. Disruption of intracellular Zn²⁺ ion may be associated with numerous diseases including Parkinson's syndrome, arteriosclerosis and immunodeficiency.^[19–21] Due to the importance of these ions in biological activity, to develop simple and sensitive methods for detecting Cu²⁺, Hg²⁺, and Zn²⁺ will be of great significance.

Researchers have developed a variety of mature methods in the detection of metal ions, such as Atomic Absorption Spectroscopy (AAS), Atomic Emission Spectrometry (AES) and Inductively Coupled Plasma Mass Spectrometry (ICP-MS), etc.^[22–25] However, these traditional methods have some disadvantages such as pretreatment of samples, slow detection speed, and expensive detection costs. In recent years, peptide-based fluorescent sensors for the detection of metal ions have received considerable attention. As important small biological molecules, peptides have the advantages of simple and well-developed synthetic methods with low costs, and can provide multidentate coordination to metal ions, etc. Peptide-based sensors have high sensitivity and high selectivity to metal ions

CONTACT Lianzhi Li  lilianzhi1963@163.com  School of Chemistry and Chemical Engineering, Liaocheng University, Liaocheng 252059, P. R. China.

 Supplemental data for this article can be accessed online at <http://dx.doi.org/10.1080/00387010.2022.2101477>.

© 2022 Taylor & Francis Group, LLC

and can be further optimized by adjusting the peptide sequence. Compared with other types of sensors, peptide-based metal ion sensors have good water solubility, biocompatibility, and low toxicity, and therefore have important applications in environmental detection and bioanalytical diagnosis.^[26–28] Therefore, we designed a peptide-based sensor fluorescence sensor. To date, some peptide-based fluorescence sensors for detecting Cu^{2+} , Hg^{2+} and Zn^{2+} ions have been reported.^[29–39] Most of the reported methods are single metal detection, and few multianalyte peptide fluorescent sensors for the simultaneous detection of three different metal ions have been reported.

In this work, a peptide-based fluorescence sensor (Dansyl-His-Thr-Glu-His-Trp-NH₂, D-P5) was synthesized. His containing imidazole group and Glu containing carboxyl group can interact with several heavy metal ions such as Ag^+ , Cu^{2+} , Zn^{2+} and Hg^{2+} . Moreover, the exogenous fluorescent group Dansyl and the endogenous fluorescent group tryptophan (Trp) are used as signal markers. Dansyl chloride is a strong fluorescent agent commonly used in the modification of peptide and protein because it can react specifically with primary amino groups at the N-terminal of peptide chain to produce a stable and strong fluorescent sulfonamide adduct of dansyl-peptide. Therefore, in this paper, we have designed a dansyl modified peptide as a metal ion sensor by combining the advantages of the strong fluorescence of dansyl group and the metal ion binding property of peptide. Through the measurement of fluorescence spectra, D-P5 showed different types of fluorescence responses to the three metal ions of Cu^{2+} , Hg^{2+} and Zn^{2+} . The calculated binding constants were $3.23 \times 10^5 \text{ L} \cdot \text{mol}^{-1}$, $6.37 \times 10^5 \text{ L} \cdot \text{mol}^{-1}$ and $6.0 \times 10^4 \text{ L} \cdot \text{mol}^{-1}$, respectively, which indicated that D-P5 has a high affinity for Cu^{2+} , Hg^{2+} and Zn^{2+} . In addition, the D-P5 sensor can be applied to the detection of metal ions in real water samples.

Materials and experimental

Materials and instruments

Rink amide resin, Fmoc-Glu(OtBu)-OH, Fmoc-Thr(tBu)-OH, Fmoc-His(Trt)-OH and Fmoc-Trp(Boc)-OH were purchased from CS Bio. Co.,

USA. Dansyl chloride, trifluoroacetic (TFA), Triisopropylsilane (TIS) and N,N-diisopropylethylamine (DIEA) were obtained from Shanghai Macklin Biochemical Co., Ltd. Stock solutions of metal ions ($10 \text{ mmol} \cdot \text{L}^{-1}$) were prepared with nitrate or chloride salts in distilled water, including Na^+ , K^+ , Ba^{2+} , Cr^{3+} , Ca^{2+} , Mn^{2+} , Co^{2+} , Ni^{2+} , Fe^{3+} , Zn^{2+} , Cd^{2+} , Hg^{2+} , Cu^{2+} , Pb^{2+} , Mg^{2+} and Al^{3+} , and various anion solutions (F^- , Cl^- , Br^- , I^- , PO_4^{3-} , NO_3^- , SO_4^{2-} , ClO_4^- and Ac^-) were prepared with the same concentration of sodium or potassium salts.

CS 136 Peptide Synthesizer (CS Bio Co., USA), API 4500 QTRAP Mass Spectrometer (Applied Biosystems/MDS SCIEX, USA), Hitachi F-7000 fluorescence spectrofluorometer (Hitachi Inc., Japan), Jasco J-810 Spectropolarimeter (Jasco Corp., Japan), Hitachi UH-4150 spectrophotometer (Hitachi Inc., Japan).

Synthesis of peptide-based sensor

Based on our previous reports,^[40–43] D-P5 was synthesized by standard Fmoc solid-phase synthesis. According to the peptide sequence (Dansyl-His-Thr-Glu-His-Trp), the Fmoc-amino acids (0.6 mmol) were sequentially coupled to the Rink Amide resin (0.2 mmol) from the C-terminus to the N-terminus. Then, after deprotecting the Fmoc group, 0.6 mmol dansyl chloride was added. The formed peptide and protecting groups were cleaved from the Rink Amide resin by treatment with a mixture of 6 mL TFA:TIS:H₂O (95:2.5:2.5, v/v/v) at room temperature for 4 h (Fig. S1). Finally, the peptide was extracted in ether at -20°C and centrifuged at 10,000 rpm for 5 min at -4°C . ESI-MS (m/z) of L calculated value: 940.4; Observed value: 941. 3 ($[\text{M} + \text{H}]^+$); 985.3 ($[(\text{M}-2\text{H}^+)+2\text{Na}^++\text{H}]^+$) (Fig. S2).

General fluorescence measurements

D-P5 was dissolved in distilled water to prepare a $3.0 \text{ mmol} \cdot \text{L}^{-1}$ stock solution. A certain amount of D-P5 stock solutions were added to the distilled water (pH 7.4) to prepare solutions of the desired concentration. The fluorescence emission spectra of D-P5 sensor were measured in the presence of 16 kinds of metal ions (Na^+ , K^+ , Ba^{2+} , Cr^{3+} ,

Ca^{2+} , Mn^{2+} , Co^{2+} , Ni^{2+} , Fe^{3+} , Zn^{2+} , Cd^{2+} , Hg^{2+} , Cu^{2+} , Pb^{2+} , Mg^{2+} and Al^{3+}) and 9 kinds of anions (F^- , Cl^- , Br^- , I^- , PO_4^{3-} , NO_3^- , SO_4^{2-} , ClO_4^- and Ac^-). Measurement conditions: $\lambda_{\text{ex}} = 295 \text{ nm}$, $\lambda_{\text{em}} = 330 \text{ nm}$; Scan speed: 1200 nm/min .

The pH values of the sample solutions were adjusted by addition of different amounts of HCl or NaOH solutions. Fluorescence emission spectra of D-P5 and D-P5-Cu/Hg/Zn system were determined at various pH values with excitation wavelength of 330 nm .

Job's plot

A series of solutions containing 0, 2, 4, 6, 8, 10, 12, 14, 16, 18 and $20 \mu\text{mol}\cdot\text{L}^{-1}$ D-P5 and 20, 18, 16, 14, 12, 10, 8, 6, 4, 2 and $0 \mu\text{mol}\cdot\text{L}^{-1}$ metal ions (Cu^{2+} , Hg^{2+} , Zn^{2+}), respectively, were prepared. These solutions kept different molar concentration ratio of D-P5 to Cu^{2+} , Hg^{2+} , and Zn^{2+} and to make the total concentration at $20 \mu\text{mol}\cdot\text{L}^{-1}$. The fluorescence emission spectra of these solution were measured at excitation wavelength of 330 nm , and the scan speed was 1200 nm/min .

Binding constants of peptide-based sensor to copper(II), mercury(II) and zinc(II)

Based on the fluorescence titration experiments of D-P5 with Cu^{2+} , Hg^{2+} and Zn^{2+} , the binding constants of D-P5 with Cu^{2+} , Hg^{2+} and Zn^{2+} were calculated according to the Benesi-Hildebrand equation:^[37]

$$\Delta FI_{\text{max}}/\Delta FI = 1 + ([M]^{-n}/K)$$

$\Delta FI_{\text{max}} = FI_{\text{max}} - FI_0$, $\Delta FI = FI_x - FI_0$, FI_{max} is the maximal fluorescence intensity of D-P5 in the absence of metal ions, FI_0 is the fluorescence intensity of D-P5 in the absence of metal ions, FI_x is the fluorescence intensity of D-P5 in the presence of different concentrations of Cu^{2+} , Hg^{2+} and Zn^{2+} , $[M]$ is the added concentration of Cu^{2+} , Hg^{2+} and Zn^{2+} , K is the binding constant of D-P5 sensor with Cu^{2+} , Hg^{2+} and Zn^{2+} .

Determination of detection limits for copper(II), mercury(II) and zinc(II)

The detection limits of D-P5 for Cu^{2+} , Hg^{2+} , Zn^{2+} were determined based on the titration curves of D-P5 with Cu^{2+} , Hg^{2+} , Zn^{2+} . The fluorescence emission intensity of D-P5 was measured ten times and then the standard deviation of blank measurement was determined. According to the titration experiment, the fluorescence intensities corresponding to different Cu^{2+} , Hg^{2+} , and Zn^{2+} concentrations were linearly fitted to determine the slope. The detection limits were obtained according to the following formula: $LOD = 3SD/m$. SD represents the standard deviation of the blank, and m represents the slope of the linear fitting line.

Ultraviolet and circular dichroism spectra measurements

Ultraviolet absorption spectra and circular dichroism (CD) spectra of D-P5 samples were determined in distilled water (pH 7.4). CD spectra of D-P5 were recorded between 200 nm and 330 nm in a 1 cm path length quartz optical cell with the scanning speed of 500 nm/min .

Results and discussion

Fluorescence response of peptide-based sensor to metal ion and anion

The prepared peptide-based sensor showed good stability measured by the absorption spectra. The fluorescence spectra of D-P5 were measured under excitation at 295 nm and 330 nm , and the fluorescence response changes of D-P5 in the presence of 16 metal ions and 9 anions were measured. As shown in Fig. 1a, D-P5 had two strong fluorescence emission peaks at 360 nm and 550 nm at an excitation wavelength of 295 nm , respectively. The emission peak at 360 nm is the fluorescence response of tryptophan (Trp), and the emission peak at 550 nm is the fluorescence response of Dansyl. When different metal ions and anions were added, the presence of Cu^{2+} reduced the fluorescence intensity of the Trp and Dansyl; the presence of Hg^{2+} caused the intensity decrease of the Trp and the U-shaped intensity

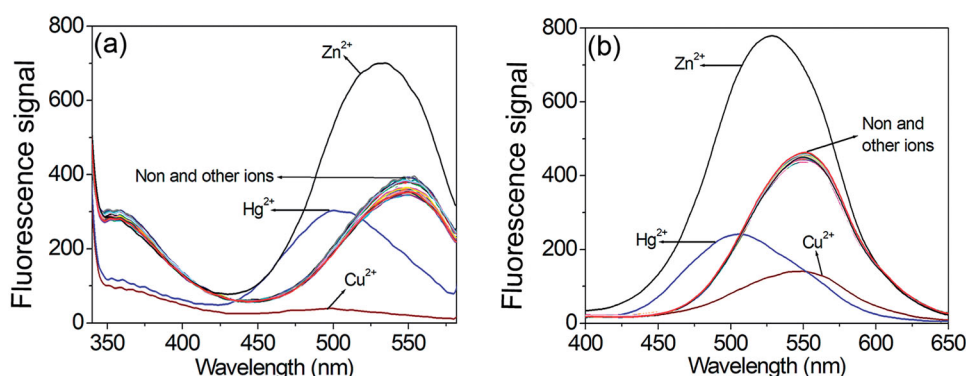


Figure 1. Fluorescence emission spectra of peptide-based sensor in the presence of different metal ions and anions. The spectra reveal the change of fluorescence signal induced by different metal ions and anions, aiming to measure the selectivity of the sensor for metal ions: (a) excitation wavelength: 295 nm; (b) excitation wavelength: 330 nm. Cu^{2+} : copper(II); Hg^{2+} : mercury(II); Zn^{2+} : zinc(II); concentrations of the sensor: $10\ \mu\text{mol}\cdot\text{L}^{-1}$; concentrations of metal ions and anions: $33.3\ \mu\text{mol}\cdot\text{L}^{-1}$.

decrease of the Dansyl; the addition of Zn^{2+} caused the Trp intensity to decrease and the intensity of Dansyl peak was strongly enhanced with a blue shift of 15 nm. Since Cu^{2+} is a paramagnetic substance, the inherent mechanism of the paramagnetic substance will quench the fluorophore, so it exhibited an obvious quenching effect.^[44] Cu^{2+} can also act as a quencher for the electron transfer process. In the presence of Hg^{2+} , the fluorescence intensities of the Trp and the Dansyl groups were decreased, and the emission peak of Dansyl group was blue-shifted. It is possible that the excited Dansyl group transfers electrons to mercury, which caused the fluorescence intensity to be quenched.^[35] The addition of Zn^{2+} may cause the folding of D-P5 by binding with the amino acid residues of the peptide chain to bring the Trp group (Donor) and the Dansyl group (receptor) closer, thereby generating a fluorescence resonance energy transfer (FRET) effect from donor Trp to receptor Dansyl group.^[39]

When excited at 330 nm, D-P5 had a strong fluorescence response at 550 nm (Fig. 1b). D-P5 had the special fluorescence response to Cu^{2+} , Hg^{2+} and Zn^{2+} among various ions, and the fluorescence intensity changes were similar to those at 295 nm excitation. The result can further explain that the inherent paramagnetic mechanism of Cu^{2+} is the main factor leading to the quenching of fluorescence intensity;^[11] in the presence of Hg^{2+} , it is possible that the excited Dansyl transfers electrons to the mercury, resulting in a decrease in the intensity of the Dansyl

peak at 550 nm;^[35,43] the addition of Zn^{2+} may destroyed photoinduced electron transfer (PET) process and caused the fluorescence intensity to recover.^[33,38] The results showed that the micro-environment of Dansyl in the solution is easily disturbed by the three metal ions.

Fluorescence titration in the presence of different concentrations of copper(II), mercury(II) and zinc(II)

Under the conditions of $\lambda_{\text{ex}} = 295\ \text{nm}$ and $\lambda_{\text{ex}} = 330\ \text{nm}$, respectively, fluorescence titrations were measured for Cu^{2+} , Hg^{2+} and Zn^{2+} at different concentrations. Fig. 2 shows the fluorescence titration measurements of $10.0\ \mu\text{mol}\cdot\text{L}^{-1}$ D-P5 with $0\text{--}7.3\ \mu\text{mol}\cdot\text{L}^{-1}$ Cu^{2+} . As shown in Fig. 2a, the fluorescence intensity of Trp and Dansyl gradually decreased ($\lambda_{\text{ex}} = 295\ \text{nm}$). The intensity of Dansyl at 550 nm also decreased with the increased Cu^{2+} concentration under 330 nm excitation (Fig. 2b). The result showed that Cu^{2+} had an inherent quenching mechanism to D-P5, so Cu^{2+} can be used as a quencher for D-P5.

As shown in Fig. 3a, with the increased concentration of Hg^{2+} ($0\text{--}4.6\ \mu\text{mol}\cdot\text{L}^{-1}$), the fluorescence intensity of Trp gradually decreased, and the intensity of Dansyl decreased with a blue shift under the excitation wavelength of 295 nm. When $\lambda_{\text{ex}} = 330\ \text{nm}$ (Fig. 3b), the intensity of Dansyl also decreased in a U-shape with a blue shift from 550 nm to 490 nm. The significant blue-shift of the maximum emission observed at high Hg^{2+} concentrations could be attributed to

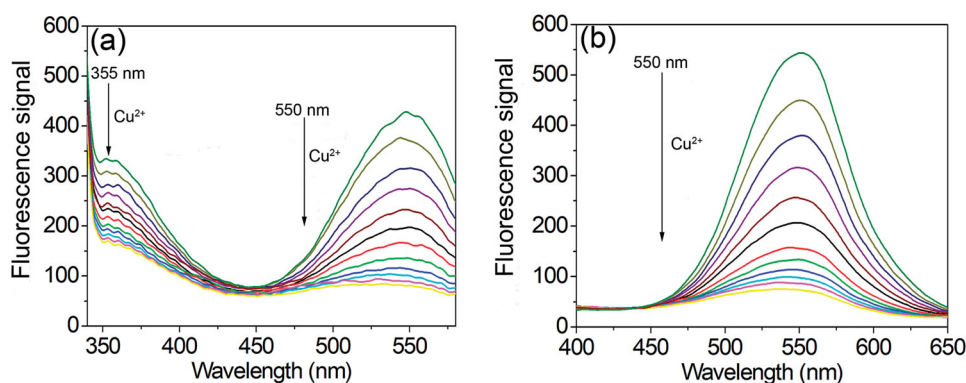


Figure 2. Fluorescence emission spectra of peptide-based sensor with different concentrations of copper(II) ion. The spectra show the change of fluorescence signal induced by copper(II) ion; (a) excitation wavelength: 295 nm; (b) excitation wavelength: 330 nm. Cu^{2+} : copper(II); concentrations of the sensor: $10 \mu\text{mol}\cdot\text{L}^{-1}$; concentrations of copper(II): $0\text{--}7.3 \mu\text{mol}\cdot\text{L}^{-1}$ from top to bottom.

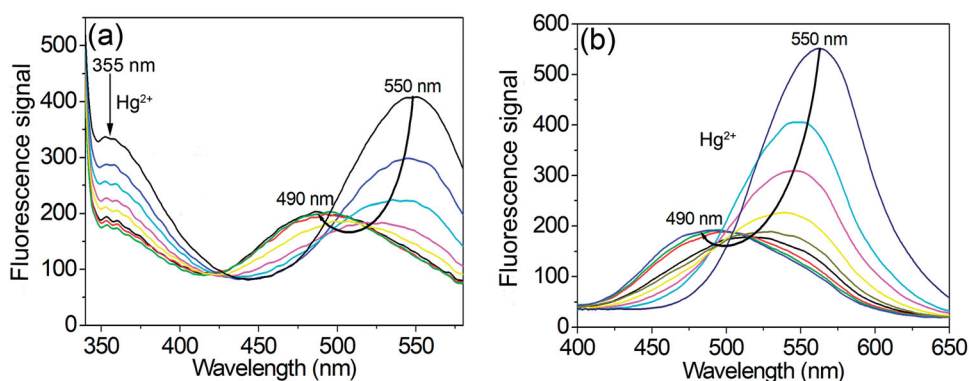


Figure 3. Fluorescence emission spectra of peptide-based sensor with different concentrations of mercury(II) ion. The spectra show the change of fluorescence signal induced by mercury(II) ion; (a) excitation wavelength: 295 nm; (b) excitation wavelength: 330 nm. Hg^{2+} : mercury(II); concentrations of the sensor: $10 \mu\text{mol}\cdot\text{L}^{-1}$; concentrations of mercury(II): $0\text{--}4.6 \mu\text{mol}\cdot\text{L}^{-1}$ from top to bottom.

the deprotonation of the dansyl-sulfonamide moiety upon binding to the strongly electrophilic Hg^{2+} ion. In this complex, deprotonation and direct binding of the NH group of the sulfonamide to Hg^{2+} was always accompanied by a blue shift in the emission due to the reduced conjugation between the deprotonated sulfonamide and the (dimethylamino)naphthalene moiety.^[45]

When $\lambda_{\text{ex}} = 295 \text{ nm}$, the fluorescence intensity of Trp (donor) gradually weakened with the increase of Zn^{2+} concentration ($0\text{--}33.3 \mu\text{mol}\cdot\text{L}^{-1}$), while the fluorescence intensity of Dansyl gradually enhanced, and blue shifts from 550 nm to 505 nm (Fig. 4a). It can be inferred that it occurred a FRET from Trp to Dansyl group. Furthermore, when the excitation wavelength was at 330 nm , the fluorescence intensity of Dansyl gradually increases with the increase of Zn^{2+} concentration (Fig. 4b). The ‘turn on’ response indicated that the PET process was disrupted, leading to the recovery of fluorescence intensity. Table 1 lists some

different sensor mechanisms for detecting Cu^{2+} , Hg^{2+} and Zn^{2+} ions.

pH effects

In order to test the ability of the D-P5 sensor to detect Cu^{2+} , Hg^{2+} and Zn^{2+} ions, the effects of pH values on the fluorescence spectra of D-P5 and D-P5-Cu/Hg/Zn systems were studied (Fig. 5). When the pH was from 1.0 to 5.0, the fluorescence intensities of D-P5 and D-P5-Cu/Hg/Zn systems at 550 nm were weak. The reason is that D-P5 and D-P5-Cu/Hg/Zn systems were in protonated state under acidic conditions, which hinders the charge transfer between the dimethylamino group ($\text{pK}_{\text{a}} \sim 4$) and the naphthalene ring, resulting in weaker fluorescence intensity.^[52–54] When in the pH range from 5 to 13, the alkalinity of the solution increases the negative charge of the imidazole on the His residue and the carboxyl group on the Glu residue

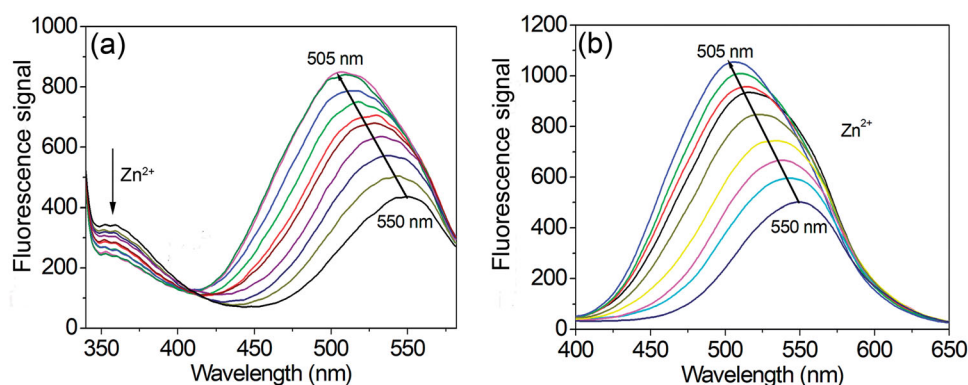


Figure 4. Fluorescence emission spectra of peptide-based sensor with different concentrations of zinc(II) ion. The spectra show the change of fluorescence signal induced by zinc(II) ion: (a) concentrations of zinc(II): 0–4.6 $\mu\text{mol}\cdot\text{L}^{-1}$ from bottom to top; excitation wavelength: 295 nm. (b) concentrations of zinc(II): 0–33.3 $\mu\text{mol}\cdot\text{L}^{-1}$ from bottom to top; excitation wavelength: 330 nm.

Table 1. Various sensing mechanisms for detecting copper(II), mercury(II) and zinc(II) ions.

Detection agent	Detection ion	Mechanism/Phenomenon	References
Dansyl-GC	Copper(II)	Paramagnetism quenching	[11]
Dansyl-HKH-Dansyl			[33]
Dansyl-ECEW			[37]
Dansyl-SPGH			[38]
FITC-SSH	Mercury(II)	Blue Shift	[46]
Dansyl-CC-Dansyl			[17]
Dansyl-HPGW			[35]
Dansyl-Met			[47]
Dansyl-Y	Zinc(II)	Fluorescence resonance energy transfer	[48]
Dansyl-MH			[49]
Dansyl-ECEW			[37]
Dansyl-HQRTWH			[39]
Dansyl-HPGHWG		Photoinduced electron transfer	[50]
Dansyl-HKH-Dansyl			[33]
Dansyl-SPGH			[38]
Dansyl-KHG			[51]
Dansyl-SPGH		Chelation enhanced fluorescence	[38]
Dansyl-HPGHWG			[50]

Dansyl-GC: Dansyl-Gly-Cys; Dansyl-HKH-Dansyl: Dansyl-His-Lys-His-Dansyl; Dansyl-ECEW: Dansyl-Glu-Cys-Glu-Trp; Dansyl-SPGH: Dansyl-Ser-Pro-Gly-His; FITC-SSH: Fluorescein 5-isothiocyanate-Ser-Ser-His; Dansyl-CC-Dansyl: Dansyl-Cys-Cys-His-Dansyl; Dansyl-HPGW: Dansyl-His-Pro-Gly-Trp; Dansyl-Y: Dansyl-Tyr; Dansyl-MH: Dansyl-Met-His; Dansyl-HQRTWH: Dansyl-His-Gln-Arg-Thr-His-Trp; Dansyl-HPGHWG: Dansyl-His-Pro-Gly-His-Trp-Gly; Dansyl-KHG: Dansyl-Lys-His-Gly.

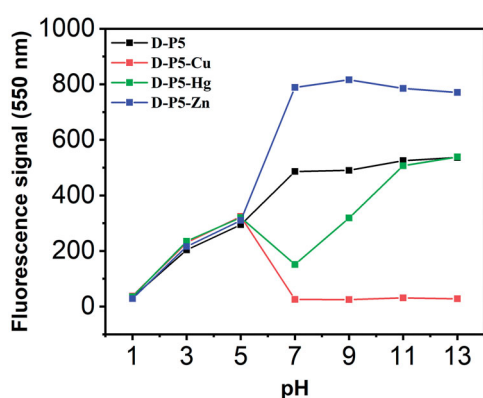


Figure 5. Fluorescence intensities at 550 nm of peptide-based sensor in the absence and presence of copper(II) (1 equiv.), mercury(II) (1 equiv.) and zinc(II) (1 equiv.) ions at different pH values. The curves show the change of fluorescence signal induced by pH value. Fl_{550} : fluorescence signal at 550 nm; D-P5: Dansyl-His-Thr-Glu-His-Trp-NH₂; D-P5-Cu: Dansyl-His-Thr-Glu-His-Trp-NH₂—copper(II); D-P5-Hg: Dansyl-His-Thr-Glu-His-Trp-NH₂—mercury(II); D-P5-Zn: Dansyl-His-Thr-Glu-His-Trp-NH₂—zinc(II); concentration of the sensor: 10 $\mu\text{mol}\cdot\text{L}^{-1}$.

in D-P5, thereby promoting the interaction of D-P5 with Cu^{2+} , Hg^{2+} , and Zn^{2+} . The overall analysis results showed that the fluorescent peptide sensor D-P5 can effectively detect Cu^{2+} , Hg^{2+} , and Zn^{2+} in a neutral environment.

Binding ability of peptide-based sensor with copper(II), mercury(II) and zinc(II)

The chemical binding ratios of D-P5 to Cu^{2+} , Hg^{2+} and Zn^{2+} through job's plot experiments were investigated. As shown in Fig. 6a, as the molar ratio of Cu^{2+} increased, the intensity of the emission peak at 550 nm gradually decreased, the fluorescence response has an inflection point when the ratio is at 0.5. The result demonstrated that D-P5 formed a 1:1 complex with Cu^{2+} . Similarly, Fig. 6b, c demonstrated that D-P5 forms a 1:1 complex with Hg^{2+} and Zn^{2+} , respectively.

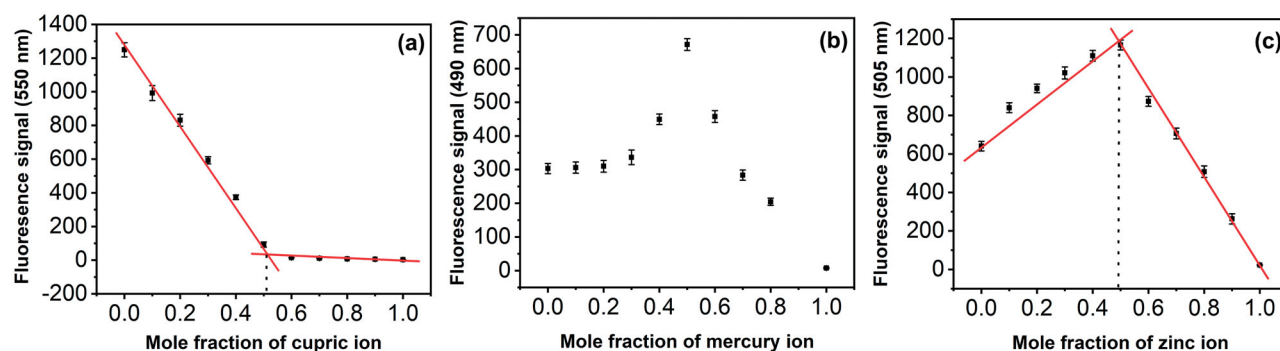


Figure 6. (a) Job's plot for determining the stoichiometry of peptide-based sensor with copper(II) ion. FI (550 nm): fluorescence signal at 550 nm; the total concentration of the sensor and copper(II) ion was $20.0 \mu\text{mol}\cdot\text{L}^{-1}$; excitation wavelength: 330 nm. (b) Job's plot for determining the stoichiometry of peptide-based sensor with mercury(II) ion. FI (550 nm): fluorescence signal at 490 nm; the total concentration of the sensor and mercury(II) ion was $20.0 \mu\text{mol}\cdot\text{L}^{-1}$; excitation wavelength: 330 nm. (c) Job's plot for determining the stoichiometry of peptide-based sensor with zinc(II) ion. FI (550 nm): fluorescence signal at 505 nm; the total concentration of the sensor and zinc(II) ion was $20.0 \mu\text{mol}\cdot\text{L}^{-1}$; excitation wavelength: 330 nm.

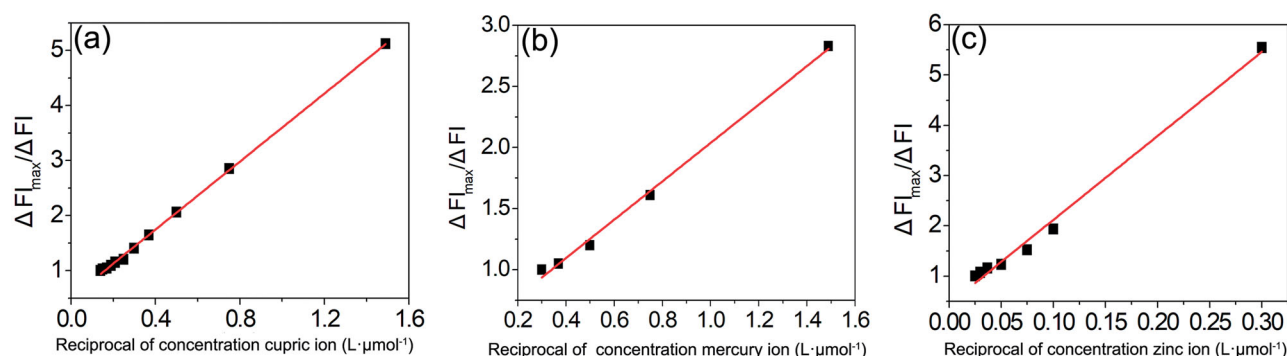


Figure 7. (a) Benesi-Hildebrand plot for the determination of the binding constant of peptide-based sensor with copper(II) ion. $\Delta F_{\text{max}} = F_{\text{max}} - F_0$, $\Delta F = F_x - F_0$, F_{max} is the maximal fluorescence intensity of the sensor in the absence of copper(II) ion, F_0 is the fluorescence intensity of the sensor in the absence of copper(II) ion, F_x is the fluorescence intensity of the sensor in the presence of different concentrations of copper(II) ion. Concentration of the sensor: $10 \mu\text{mol}\cdot\text{L}^{-1}$; excitation wavelength was 330 nm. (b) Benesi-Hildebrand plot for the determination of the binding constant of peptide-based sensor with mercury(II) ion. $\Delta F_{\text{max}} = F_{\text{max}} - F_0$, $\Delta F = F_x - F_0$, F_{max} is the maximal fluorescence intensity of the sensor in the absence of mercury(II) ion, F_0 is the fluorescence intensity of the sensor in the absence of mercury(II) ion, F_x is the fluorescence intensity of the sensor in the presence of different concentrations of mercury(II) ion. Concentration of the sensor: $10 \mu\text{mol}\cdot\text{L}^{-1}$; excitation wavelength was 330 nm. (c) Benesi-Hildebrand plot for the determination of the binding constant of peptide-based sensor with zinc(II) ion. $\Delta F_{\text{max}} = F_{\text{max}} - F_0$, $\Delta F = F_x - F_0$, F_{max} is the maximal fluorescence intensity of the sensor in the absence of zinc(II) ion, F_0 is the fluorescence intensity of the sensor in the absence of zinc(II) ion, F_x is the fluorescence intensity of the sensor in the presence of different concentrations of zinc(II) ion. Concentration of the sensor: $10 \mu\text{mol}\cdot\text{L}^{-1}$; excitation wavelength was 330 nm.

The job's plot showed that D-P5 forms a 1:1 complex with all three metal ions.

In addition, based on the fluorescence titration experiments of D-P5 with the three metal ions, the binding constants of D-P5 with Cu^{2+} , Hg^{2+} and Zn^{2+} were further studied (Fig. 7). Based on the Benesi-Hildebrand curves, the binding constants of D-P5 and Cu^{2+} , Hg^{2+} and Zn^{2+} were calculated as $3.23 \times 10^5 \text{ L}\cdot\text{mol}^{-1}$ ($R^2 = 0.9989$), $6.37 \times 10^5 \text{ L}\cdot\text{mol}^{-1}$ ($R^2 = 0.9952$) and $6.0 \times 10^4 \text{ L}\cdot\text{mol}^{-1}$ ($R^2 = 0.9911$), respectively. The overall results showed that D-P5 had a high binding affinity to the three metal ions.

Detection limit of peptide-based sensor for copper(II), mercury(II) and zinc(II)

Based on the fluorescence titration experiments, the detection limits of the peptide sensor for the three metal ions were calculated. Fig. 8 shows the linear fitting curves for titrations of D-P5 with different concentrations of Cu^{2+} , Hg^{2+} and Zn^{2+} , and the correlation coefficients of the fitted curves were $R^2 = 0.9900$, $R^2 = 0.9891$, $R^2 = 0.9919$, respectively. When the concentrations of Cu^{2+} , Hg^{2+} and Zn^{2+} were in the range of $0\text{--}10 \mu\text{mol}\cdot\text{L}^{-1}$, the fluorescence intensities had a good linear relationship with

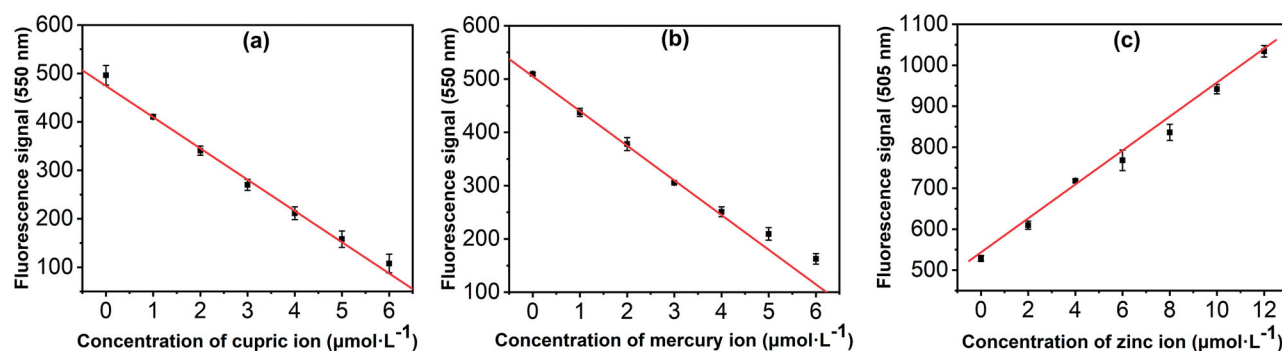


Figure 8. (a) Fluorescence intensity at 550 nm of peptide-based sensor as a function of copper(II) ion concentration for the measurement of limit of determination. (b) Fluorescence intensity at 550 nm of peptide-based sensor as a function of mercury(II) ion concentration for the measurement of limit of determination. (c) Fluorescence intensity at 550 nm of peptide-based sensor as a function of zinc(II) ion concentration for the measurement of limit of determination. F_{550} : fluorescence signal at 510 nm; concentration of the sensor— $10.0\ \mu\text{mol}\cdot\text{L}^{-1}$; excitation wavelength: 330 nm.

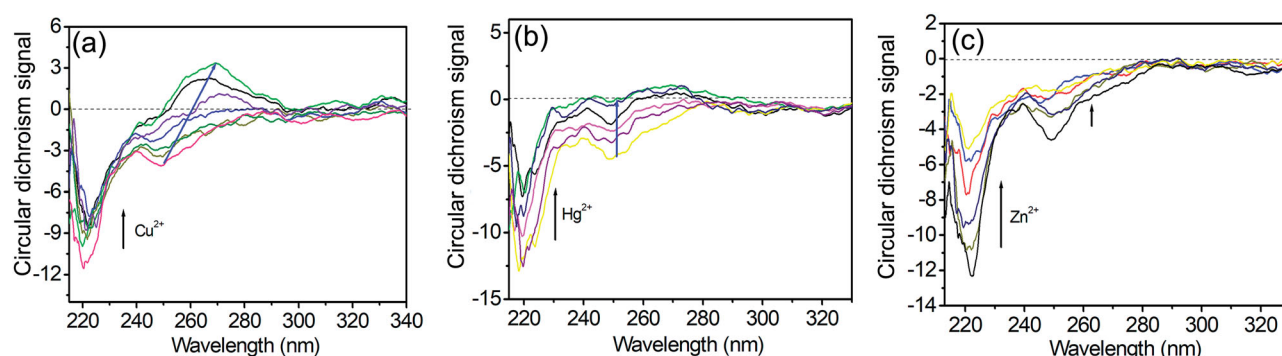


Figure 9. (a) Circular dichroism spectra of peptide-based sensor in the presence of different copper(II) concentrations. Concentration of the sensor— $50.0\ \mu\text{mol}\cdot\text{L}^{-1}$; copper(II) concentrations— 0 – $20\ \mu\text{mol}\cdot\text{L}^{-1}$ from bottom to top. (b) Circular dichroism spectra of peptide-based sensor in the presence of different mercury(II) concentrations. Concentration of the sensor— $50.0\ \mu\text{mol}\cdot\text{L}^{-1}$; mercury(II) concentrations— 0 – $9.3\ \mu\text{mol}\cdot\text{L}^{-1}$ from bottom to top. (c) Circular dichroism spectra of peptide-based sensor in the presence of different zinc(II) concentrations. Concentration of the sensor— $50.0\ \mu\text{mol}\cdot\text{L}^{-1}$; zinc(II) concentrations— 0 – $46.6\ \mu\text{mol}\cdot\text{L}^{-1}$ from bottom to top.

metal ion concentration. The detection limits of D-P5 for Cu^{2+} , Hg^{2+} and Zn^{2+} were calculated by the formula $\text{LOD} = 3\text{SD}/m$ to be $37.6\ \text{nmol}\cdot\text{L}^{-1}$, $37.8\ \text{nmol}\cdot\text{L}^{-1}$, and $59.4\ \text{nmol}\cdot\text{L}^{-1}$, respectively. The result indicates that D-P5 has a high sensitivity for the detection of three metal ions.

Ultraviolet and circular dichroism spectra of peptide-based sensor in the presence of copper(II), mercury(II) and zinc(II)

The interactions of D-P5 with different concentrations of Cu^{2+} , Hg^{2+} and Zn^{2+} were studied through the ultraviolet absorption spectrum. As shown in Fig. S3, the peak at 220 nm was mainly the characteristic absorption peak of the amide bond, while the peak at 330 nm corresponded to the characteristic absorption peak of Dansyl

group. With the increasing concentration of the three metal ions, the absorption peaks at 220 nm and 330 nm gradually decreased. It can be inferred that D-P5 may pass through the sulfonamide group of the Dansyl fluorophore and the side chain group of amino acid residues (such as histidine) chelated with Cu^{2+} , Hg^{2+} and Zn^{2+} .

Circular dichroism (CD) spectroscopy is commonly used to analyze the conformational changes of biological molecules. Therefore, circular dichroism spectroscopy was used to analyze the conformational effects of Cu^{2+} , Hg^{2+} and Zn^{2+} on D-P5. As shown in Fig. 9, the CD spectrum of D-P5 was mainly composed of two negative absorption peaks at 225 nm and 245 nm. As the concentrations of the three metal ions continue to increase, the intensities of the two peaks also gradually decreased. Meanwhile, the addition

of Cu^{2+} not only caused the peak intensity to decrease, but also became a positive absorption peak. Through the analysis of CD spectra, it is speculated that D-P5 interacted with Cu^{2+} , Hg^{2+} and Zn^{2+} , resulting in a huge change in the conformation of D-P5.

Application for the determination of lake water samples

In order to further study the application of D-P5 in real water sample detection, this sensor was used to detect Cu^{2+} , Hg^{2+} and Zn^{2+} in lake water ($\text{pH} = 7$). The standard curves were obtained by adding Cu^{2+} , Hg^{2+} and Zn^{2+} to distilled water, and then add Cu^{2+} , Hg^{2+} and Zn^{2+} to the lake water sample solution to determine the recovery rate. The standard curves are shown in Fig. S4. The results showed that the recovery rate were 95.1% for Cu^{2+} , 104.4% for Hg^{2+} and 101.3% for Zn^{2+} in the range of $1\text{--}3\ \mu\text{mol}\cdot\text{L}^{-1}$, and it can be used to measure the concentration of Cu^{2+} , Hg^{2+} and Zn^{2+} in water samples.

Conclusion

In this study, a new peptide-based sensor (Dansyl-His-Thr-Glu-His-Trp- NH_2 , D-P5) was designed and synthesized through the Fmoc solid-phase peptide synthesis method. The fluorescent peptide sensor showed different types of fluorescence responses to Cu^{2+} , Hg^{2+} and Zn^{2+} ions with good selectivity over the other metal ions examined. D-P5 had a higher binding constants for Cu^{2+} , Hg^{2+} and Zn^{2+} , respectively, which can be used to detect three metal ions of Cu^{2+} , Hg^{2+} and Zn^{2+} with lower detection limits. Compared with other reported fluorescence sensors, the peptide-based sensor was a multianalyte fluorescent sensor by monitoring the changes in fluorescence spectral in different sensing patterns. The detection limits of D-P5 for Cu^{2+} (37.6 nM), Hg^{2+} (37.8 nM) and Zn^{2+} (59.4 nM) were lower than that of the other literature. Importantly, it can be easily distinguished these three ions by fluorescence effect of D-P5, thus achieving the detection of these three ions. In addition, it could be used for the detection of real lake water. Therefore, this work has an important significance for the establishment of peptide-based fluorescent sensors for multi-ion

detection in environmental systems via different mechanisms.

Authors' contributions

Lianshun Zhang and Shuaibing Yu contributed equally. Methodology, Conceptualization, Investigation, Writing—original draft. Lei Gao: Investigation, Writing—original draft. Wei Meng: Investigation. Chen Fu: Investigation. Lianzhi Li: Resources, Supervision, Funding acquisition, Writing—review and editing.

Disclosure statement

No potential conflict of interest was reported by the author(s).

Funding

This work was supported by the Scientific Research Foundation of Liaocheng University, China [No. 318011919], and Undergraduate Training Program for Innovation and Entrepreneurship of Shandong Province, China [No. S201910447041], and the National Natural Science Foundation of China [No. 21974068].

ORCID

Lianzhi Li  <http://orcid.org/0000-0002-8447-3803>

References

- [1] Xu, J.; Cao, Z.; Zhang, Y. L.; Yuan, Z. L.; Lou, Z. M.; Xu, X. H.; Wang, X. K. A Review of Functionalized Carbon Nanotubes and Graphene for Heavy Metal Adsorption from Water: Preparation, Application, and Mechanism. *Chemosphere* **2018**, *195*, 351–364. DOI: [10.1016/j.chemosphere.2017.12.061](https://doi.org/10.1016/j.chemosphere.2017.12.061).
- [2] Hashim, M. A.; Mukhopadhyay, S.; Sahu, J. N.; Sengupta, B. Remediation Technologies for Heavy Metal Contaminated Groundwater. *Journal of Environmental Management* **2011**, *92*(10), 2355–2388. DOI: [10.1016/j.jenvman.2011.06.009](https://doi.org/10.1016/j.jenvman.2011.06.009).
- [3] Kuperman, R. G.; Carreiro, M. M. Soil Heavy Metal Concentrations, Microbial Biomass and Enzyme Activities in a Contaminated Grassland Ecosystem. *Soil Biology and Biochemistry*. **1997**, *29*(2), 179–190. DOI: [10.1016/S0038-0717\(96\)00297-0](https://doi.org/10.1016/S0038-0717(96)00297-0).
- [4] Ascenzi, P.; Tundo, G. R.; Coletta, M. The Nitrite Reductase Activity of Ferrous Human Hemoglobin: Haptoglobin 1-1 and 2-2 Complexes. *Journal of Inorganic Biochemistry* **2018**, *187*, 116–122.

- [5] Krishna, S. S.; Majumdar, I.; Grishin, N. V. Structural Classification of Zinc Fingers: Survey and Summary. *Nucleic Acids Research* **2003**, *31*(2), 532–550.
- [6] Baker, R. D.; Greer, F. R. Diagnosis and Prevention of Iron Deficiency and Iron-Deficiency Anemia in Infants and Young Children (0-3 Years of Age). *Pediatrics* **2010**, *126*(5), 1040–1050.
- [7] Zhou, F. F.; Wang, H. Q.; Liu, P. Y.; Hu, Q. H.; Wang, Y. Y.; Liu, C.; Hu, J. K. A Highly Selective and Sensitive Turn-on Probe for Aluminum(III) Based on Quinoline Schiff's Base and Its Cell Imaging. *Spectrochimica Acta. Part A, Molecular and Biomolecular Spectroscopy* **2018**, *190*, 104–110. DOI: [10.1016/j.saa.2017.09.007](https://doi.org/10.1016/j.saa.2017.09.007).
- [8] Martinez-Manez, R.; Sancenon, F. Fluorogenic and Chromogenic Chemosensors and Reagents for Anions. *Chemical Reviews* **2003**, *103*, 4419–4476.
- [9] Kim, J. S.; Quang, D. T. Calixarene-Derived Fluorescent Probes. *Chemical Reviews* **2007**, *107*(9), 3780–3799.
- [10] Kobayashi, H.; Ogawa, M.; Alford, L.; Choyke, P. L.; Urano, Y. New Strategies for Fluorescent Probe Design in Medical Diagnostic Imaging. *Chemical Reviews* **2010**, *110*(5), 2620–2640.
- [11] Wang, P.; Wu, J.; Zhao, C. H. A Water-Soluble Peptide Fluorescent Chemosensor for Detection of Cadmium (II) and Copper (II) by Two Different Response Modes and Its Application in Living LNCap Cells. *Spectrochimica Acta. Part A, Molecular and Biomolecular Spectroscopy* **2020**, *226*, 117600. DOI: [10.1016/j.saa.2019.117600](https://doi.org/10.1016/j.saa.2019.117600).
- [12] Renzoni, A.; Zino, F.; Franchi, E. Mercury Levels along the Food Chain and Risk for Exposed populations. *Environmental Research* **1998**, *77*(2), 68–72.
- [13] Koester, C. J.; Moulik, A. Trends in Environmental Analysis. *Analytical Chemistry* **2005**, *77*(12), 3737–3754.
- [14] Richardson, S. D.; Ternes, T. A. Water Analysis: Emerging Contaminants and Current Issues. *Analytical Chemistry* **2005**, *77*(12), 3807–3838.
- [15] Kim, H. N.; Ren, W. X.; Kim, J. S.; Yoon, J. Fluorescent and Colorimetric Sensors for detection of Lead, Cadmium, and Mercury Ions. *Chemical Society Reviews* **2012**, *41*(8), 3210–3244.
- [16] Nolan, E. M.; Lippard, S. J. Tools and Tactics for the Optical Detection of Mercuric Ion. *Chemical Reviews* **2008**, *108*(9), 3443–3480.
- [17] Joshi, B. P.; Lohani, C. R.; Lee, K. H. A Highly Sensitive and Selective Detection of Hg(II) in 100% Aqueous Solution with Fluorescent Labeled Dimerized Cys Residues. *Organic & Biomolecular Chemistry* **2010**, *8*(14), 3220–3226.
- [18] Zhou, N.; Chen, H.; Li, J.; Chen, L. Highly Sensitive and Selective Voltammetric Detection of Mercury(II) Using an ITO Electrode Modified with 5-Methyl-2-Thiouracil, Graphene Oxide and Gold Nanoparticles. *Microchimica Acta* **2013**, *180*(5–6), 493–499. DOI: [10.1007/s00604-013-0956-0](https://doi.org/10.1007/s00604-013-0956-0).
- [19] Bush, A. I.; Pettingell, W. H.; Multhaup, G.; Paradis, M. D.; Vonsattel, J. P.; Gusella, J. F.; Beyreuther, K.; Masters, C. L.; Tanzi, R. E. Rapid induction of Alzheimer A β Amyloid Formation by Zinc. *Science* **1994**, *265*(5177), 1464–1467. DOI: [10.1126/science.8073293](https://doi.org/10.1126/science.8073293).
- [20] Koh, J. Y.; Suh, S. W.; Gwag, B. J.; He, Y. Y.; Hsu, C. Y.; Choi, D. W. The Role of Zinc in Selective Neuronal Death after Transient Global Cerebral Ischemia. *Science* **1996**, *272*(5264), 1013–1016.
- [21] Walker, C. F.; Black, R. E. Zinc and the Risk for Infectious Disease. *Annual Review of Nutrition* **2004**, *24*, 255–275.
- [22] Faraji, M.; Yamini, Y.; Saleh, A.; Rezaee, M.; Ghambarian, M.; Hassani, R. A Nanoparticle-Based Solid-Phase Extraction Procedure Followed by Flow Injection Inductively Coupled Plasma-Optical Emission Spectrometry to Determine Some Heavy Metal Ions in Water Samples. *Analytica Chimica Acta* **2010**, *659*(1–2), 172–177. DOI: [10.1016/j.aca.2009.11.053](https://doi.org/10.1016/j.aca.2009.11.053).
- [23] Liu, Y.; Liang, P.; Guo, L. Nanometer Titanium Dioxide Immobilized on Silica Gel as Sorbent for Preconcentration of Metal Ions Prior to Their Determination by Inductively Coupled Plasma Atomic Emission Spectrometry. *Talanta* **2005**, *68*(1), 25–30. DOI: [10.1016/j.talanta.2005.04.035](https://doi.org/10.1016/j.talanta.2005.04.035).
- [24] Benvidi, A.; Yekrangi, M.; Jahanbani, S.; Zare, H. R. The Extraction and Measurement of Nickel Metal Ion in Crab, Shellfish and Rice Samples Using Magnetic Silk Fibroin – EDTA Ligand and Furnace Atomic Absorption Spectrometry. *Food Chemistry* **2010**, *659*, 172–177.
- [25] Divrikli, U.; Kartal, A. A.; Soylak, M.; Elci, L. Preconcentration of Pb(II), Cr(III), Cu(II), Ni(II) and Cd(II) Ions in Environmental Samples by Membrane Filtration Prior to Their Flame Atomic Absorption Spectrometric Determinations. *Journal of Hazardous Materials* **2007**, *145*(3), 459–464.
- [26] Pazos, E.; Vazquez, O.; Mascarenas, J. L.; Vazquez, M. E. Peptide-Based Fluorescent Biosensors. *Chemical Society Reviews* **2009**, *38*(12), 3348–3359.
- [27] Liu, Q. T.; Wang, J. F.; Boyd, B. J. Peptide-Based Biosensors. *Talanta* **2015**, *136*, 114–127. DOI: [10.1016/j.talanta.2014.12.020](https://doi.org/10.1016/j.talanta.2014.12.020).
- [28] Yu, S. B.; Wang, Z. L.; Pang, X. L.; Wang, L.; Li, L. Z.; Lin, Y. W. Peptide-Based Metal Ion Sensors. *Progress in Chemistry* **2021**, *33*, 380–393.
- [29] Joshi, B. P.; Park, J.; Lee, W. I.; Lee, K. H. Ratiometric and Turn-on Monitoring for Heavy and Transition Metal Ions in Aqueous Solution with a Fluorescent Peptide Sensor. *Talanta* **2009**, *78*(3), 903–909. DOI: [10.1016/j.talanta.2008.12.062](https://doi.org/10.1016/j.talanta.2008.12.062).
- [30] Wang, B.; Li, H. W.; Gao, Y.; Zhang, H. Y.; Wu, Y. Q. A Multifunctional Fluorescence Probe for the

- Detection of Cations in Aqueous Solution: The Versatility of Probes Based on Peptides. *Journal of Fluorescence* **2011**, 21(5), 1921–1931. DOI: [10.1007/s10895-011-0891-6](https://doi.org/10.1007/s10895-011-0891-6).
- [31] Wan, J. J.; Duan, W. X.; Chen, K.; Tao, Y. D.; Dang, J.; Zeng, K. H.; Ge, Y. S.; Wu, J.; Liu, D. Selective and Sensitive Detection of Zn(II) Ion Using a Simple Peptide-Based Sensor. *Sensors and Actuators B: Chemical* **2018**, 255, 49–56. DOI: [10.1016/j.snb.2017.08.038](https://doi.org/10.1016/j.snb.2017.08.038).
- [32] Jung, K. H.; Oh, E. T.; Park, H. J.; Lee, K. H. Development of New Peptide-Based Receptor of Fluorescent Probe with Femtomolar Affinity for Cu⁺ and Detection of Cu⁺ in Golgi Apparatus. *Biosensors and Bioelectronics*. **2016**, 85, 437–444. DOI: [10.1016/j.bios.2016.04.101](https://doi.org/10.1016/j.bios.2016.04.101).
- [33] Wang, P.; Liu, L. X.; Zhou, P. P.; Wu, W. Y.; Wu, J.; Liu, W. S.; Tang, Y. A Peptide-Based Fluorescent Chemosensor for Multianalyte Detection. *Biosensors & Bioelectronics* **2015**, 72, 80–86.
- [34] Feng, H. Y.; Gao, L.; Ye, X. H.; Wang, L.; Xue, Z. C.; Kong, J. M.; Li, L. Z. Synthesis of a Heptapeptide and Its Application in the Detection of Mercury(II) Ion. *Chemical Research in Chinese Universities* **2017**, 33(2), 155–159. DOI: [10.1007/s40242-017-6362-0](https://doi.org/10.1007/s40242-017-6362-0).
- [35] Pang, X. L.; Gao, L.; Feng, H. Y.; Li, X. D.; Kong, J. M.; Li, L. Z. A Peptide-Based Multifunctional Fluorescent Probe for Cu²⁺, Hg²⁺ and Biothiol. *New Journal of Chemistry* **2018**, 42(19), 15770–15777. DOI: [10.1039/C8NJ03624A](https://doi.org/10.1039/C8NJ03624A).
- [36] Pang, X. L.; Wang, L.; Gao, L.; Feng, H. Y.; Kong, J. M.; Li, L. Z. Multifunctional Fluorescent Peptide-Based Chemosensor for Detection of Hg²⁺, Cu²⁺ and S²⁻ Ions. *Luminescence* **2019**, 34(6), 585–594. DOI: [10.1002/bio.3641](https://doi.org/10.1002/bio.3641).
- [37] Pang, X. L.; Dong, J. F.; Gao, L.; Wang, L.; Yu, S. B.; Kong, J. M.; Li, L. Z. Dansyl-Peptide Dual-Functional Fluorescent Chemosensor for Hg²⁺ and Biothiols. *Dyes and Pigments* **2020**, 173, 107888. DOI: [10.1016/j.dyepig.2019.107888](https://doi.org/10.1016/j.dyepig.2019.107888).
- [38] Wang, P.; Xue, S. R.; Yang, X. P. A Novel Peptide-Based Fluorescent Chemosensor for Detection of Zinc (II) and Copper (II) through Differential Response and Application in Logic Gate and Bioimaging. *Microchemical Journal* **2020**, 158, 105147. DOI: [10.1016/j.microc.2020.105147](https://doi.org/10.1016/j.microc.2020.105147).
- [39] Yu, S. B.; Li, Y.; Gao, L.; Zhao, P. R.; Wang, L.; Li, L. Z.; Lin, Y. W. A Highly Selective and Sensitive Zn²⁺ Fluorescent Sensor Based on Zinc Finger-Like Peptide and Its Application in Cell Imaging. *Spectrochimica Acta. Part A, Molecular and Biomolecular Spectroscopy* **2021**, 261, 120042. DOI: [10.1016/j.saa.2021.120042](https://doi.org/10.1016/j.saa.2021.120042).
- [40] Li, Y.; Li, L. Z.; Pu, X. W.; Ma, G. L.; Wang, E. Q.; Kong, J. M.; Liu, Z. P.; Liu, Y. Z. Synthesis of a Ratiometric Fluorescent Peptide Sensor for the Highly Selective Detection of Cd²⁺. *Bioorganic & Medicinal Chemistry Letters* **2012**, 22(12), 4014–4017.
- [41] Wang, Z. L.; Feng, H. Y.; Li, Y.; Xu, T.; Xue, Z. C.; Li, L. Z. A High Selective Fluorescent Ratio Sensor for Cd²⁺ Based on the Interaction of Peptide with Metal Ion. *Chinese Journal of Inorganic Chemistry* **2015**, 31, 1946–1952.
- [42] Yu, S. B.; Wang, Z. L.; Gao, L.; Zhang, B.; Wang, L.; Kong, J. M.; Li, L. Z. A Highly Selective and Sensitive Peptide-Based Fluorescent Ratio Sensor for Ag. *Journal of Fluorescence* **2021**, 31(1), 237–246.
- [43] Yu, S. B.; Gao, L.; Li, R.; Fu, C.; Meng, W.; Wang, L.; Li, L. Z. Ultrasensitive Mercury Ion and Biothiol Detection Based on Dansyl-His-Pro-Gly-Asp-NH₂ Fluorescent Sensor. *Spectrochimica Acta. Part A, Molecular and Biomolecular Spectroscopy* **2021**, 250, 119246. DOI: [10.1016/j.saa.2020.119246](https://doi.org/10.1016/j.saa.2020.119246).
- [44] Wang, P.; Wu, J.; Su, P. S.; Xu, C.; Ge, Y. S.; Liu, D.; Liu, W. S.; Tang, Y. Fluorescence “On–Off–On” Peptide-Based Chemosensor for the Selective Detection of Cu²⁺ and S²⁻ and Its Application in Living Cell Bioimaging. *Dalton Transactions* **2016**, 45(41), 16246–16254. DOI: [10.1039/c6dt03330j](https://doi.org/10.1039/c6dt03330j).
- [45] Siepi, M.; Oliva, R.; Petraccone, L.; Vecchio, P. D.; Ricca, E.; Istitato, R.; Lanzilli, M.; Maglio, O.; Lombardi, A.; Leone, L.; et al. Fluorescent Peptide dH3w: A Sensor for Environmental Monitoring of Mercury (II). *PLOS One* **2018**, 13(10), e0204164. DOI: [10.1371/journal.pone.0204164](https://doi.org/10.1371/journal.pone.0204164).
- [46] Wang, P.; Sun, L. Y.; Wu, J.; Yang, X. P.; Lin, P. C.; Wang, M. A Dual-Functional Colorimetric and Fluorescent Peptide-Based Probe for Sequential Detection of Cu²⁺ and S²⁻ in 100% Aqueous Buffered Solutions and Living Cells. *Journal of Hazardous Materials* **2021**, 407, 124388. DOI: [10.1016/j.jhazmat.2020.124388](https://doi.org/10.1016/j.jhazmat.2020.124388).
- [47] Yang, M. H.; Lohani, C. R.; Cho, H.; Lee, K. H. A Methionine-Based Turn-On Chemical Sensor for Selectively Monitoring Hg²⁺ Ions in 100% Aqueous Solution. *Organic & Biomolecular Chemistry* **2011**, 9(7), 2350–2356.
- [48] Wang, P.; An, Y.; Wu, J. Highly Sensitive Turn-on Detection of Mercury(II) in Aqueous Solutions and Live Cells with a Chemosensor Based on Tyrosine. *Spectrochimica Acta. Part A, Molecular and Biomolecular Spectroscopy* **2020**, 230, 118004. DOI: [10.1016/j.saa.2019.118004](https://doi.org/10.1016/j.saa.2019.118004).
- [49] Neupane, L. N.; Thirupathi, P.; Jang, S.; Jang, M. J.; Kim, J. H.; Lee, K. H. Highly Selectively Monitoring Heavy and Transition Metal Ions by a Fluorescent Sensor Based on Dipeptide. *Talanta* **2011**, 85(3), 1566–1574. DOI: [10.1016/j.talanta.2011.06.052](https://doi.org/10.1016/j.talanta.2011.06.052).
- [50] Wang, P.; Wu, J.; Zhou, P. P.; Liu, W. S.; Tang, Y. A Novel Peptide-Based Fluorescent Chemosensor for Measuring Zinc Ions Using Different Excitation Wavelengths and Application in Live Cell Imaging.

- Journal of Materials Chemistry. B* **2015**, 3(17), 3617–3624. DOI: [10.1039/c5tb00142k](https://doi.org/10.1039/c5tb00142k).
- [51] Wang, P.; Wang, S. H.; Chen, L.; Wang, W. T.; Wang, B. H.; Liao, Y. W. A Novel Peptide-Based Fluorescent Probe for Sensitive Detection of zinc (II) and Its Applicability in Live Cell Imaging. *Spectrochimica Acta. Part A, Molecular and Biomolecular Spectroscopy* **2020**, 240, 118549. DOI: [10.1016/j.saa.2020.118549](https://doi.org/10.1016/j.saa.2020.118549).
- [52] In, B.; Hwang, G. W.; Lee, K. H. Highly Sensitive and Selective Detection of Al(III) Ions in Aqueous Buffered Solution with Fluorescent Peptide-Based Sensor. *Bioorganic & Medicinal Chemistry Letters* **2016**, 26(18), 4477–4482.
- [53] Metivier, R.; Leray, I.; Valeur, B. Lead and Mercury Sensing by Calixarene-Based Fluoroiono-Phores Bearing Two or four Dansyl Fluorophores. *Chemistry* **2004**, 10(18), 4480–4490. DOI: [10.1002/chem.200400259](https://doi.org/10.1002/chem.200400259).
- [54] O'Connor, N. A.; Sakata, S. T.; Zhu, H.; Shea, K. J. Chemically Modified Dansyl Probes: A Fluorescent Diagnostic for Ion and Proton Detection in Solution and in Polymers. *Organic Letters* **2006**, 8(8), 1581–1584.